

The H/σ vs σ^2 plots that were measured for this Gd are shown in Fig. 1 (H is the magnetic field and σ is the induced magnetization along the « c » axis) [8].

The effects of pressure on all of the elastic moduli at 293 K (paramagnetic phase) and 273 K (ferromagnetic phase) and on c_{33} at various intermediate temperatures were measured by the pulse superposition method [9]. Nitrogen gas was the hydrostatic pressure medium and pressure measurements were obtained from a calibrated manganin pressure cell.

The corrections to the basic data that are necessary to account for path length and density changes with pressure were made by computing the linear and volume compressibilities at each interval of pressure using the following equations:

$$(c_{ij})^p = \left[\left(\frac{f_0}{f} \right)^2 \frac{1 + (\beta_{\perp})_{\pi} (\beta_{\parallel})_{\pi}}{1 + (\beta_{\perp})_{\pi} (\beta_{\parallel})_{\pi} (\Delta p)} \right] (c_{ij})_0; \quad (1)$$

$$(c_{ij})^p = \left(\frac{f_0}{f} \right)^2 \frac{1 + (\beta_{\parallel})_{\pi} (\beta_{\perp})_{\pi} (\Delta p)}{1 + (\beta_{\parallel})_{\pi} (\beta_{\perp})_{\pi}} (c_{ij})_0; \quad (2)$$

where f_0/f_0 is the ratio of the pulse repetition rate frequencies at pressure $[p]$, to that at one atmosphere, f_0 ; $(\beta_{\perp})_{\pi}$ and $(\beta_{\parallel})_{\pi}$ are the isothermal linear compressibilities perpendicular and parallel to the « c » axis, respectively, at the start of the pressure interval denoted by $[\Delta p]$, arbitrarily chosen as 300 bar.

Results

Variation of c_{ij} with T at zero applied pressure: Curves obtained from plotting the measured c_{ij} as a function of temperature at ambient pressures are shown in Fig. 2. The effects of the paramagnetic transition on the compressional modes, c_{33} , c_{11} and Q_L , are clearly observed with c_{33} showing by far the greatest effects at $T < 330$ K. The slope inversion for the c_{33} curve occurs at (286.5 ± 1) K, which is approximately 3 K less than T_c , the measured magnetic Curie temperature. The c_{11} curve changes slope abruptly at 289 K and c_{11} is constant between 289 and 286 K, at which point there is again an abrupt change. The c_{44} and c_{66} (shear moduli) curves both change slopes abruptly at 289 K. The effects between 286 and 289.5 K are then clearly associated only with compressional modes and evidently arise from the volume changes

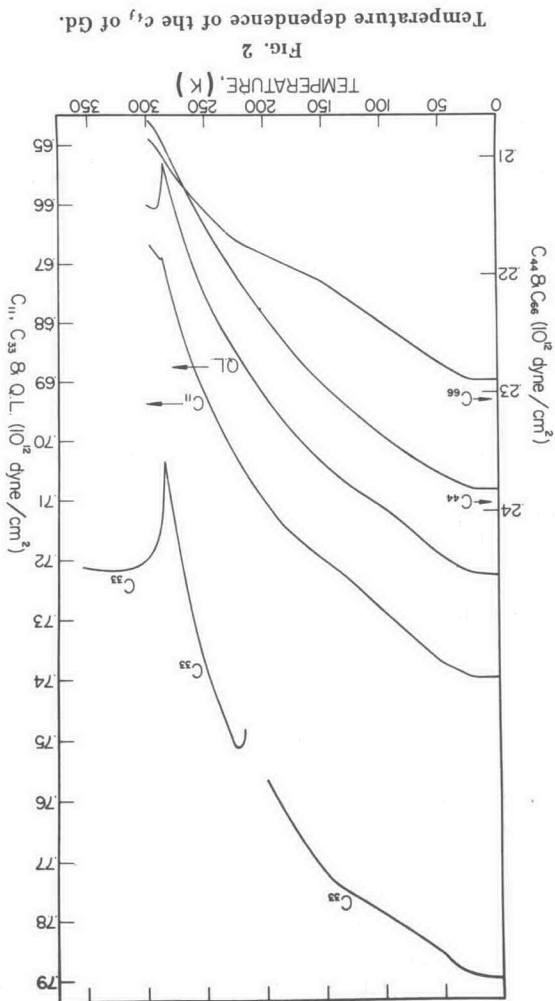


Fig. 2
Temperature dependence of the c_{ij} of Gd.

produced by the acoustic waves; i.e. shear waves do not change the volume. The much greater effect on c_{33} than c_{11} is to be expected if the modulus decrease is caused by an interaction between the strain and the magnetic anisotropy in Gd [10].

The effect on c_{33} that are implicitly due to the anomalous thermal expansion are considered in the analysis of the high pressure data. The anomaly in the c_{33} curve between 225 K and 210 K is evidently associated with the temperature change in the easy direction of magnetization and has been closely examined in a recent paper by Long et al. [2].

The adiabatic linear and volume compressibilities peak at 286 K; $(\beta_{\perp} - \beta_{\parallel})$ is positive at $T > 286$ K and negative at $T < 286$ K. *Effects of high pressure:* The results of the measurements of the changes in repetition rate frequencies with increasing hydrostatic pressure

up to 3.034 kbar, are shown in Fig. 3. These measurements were made at 298 K and 273 K, as noted in the curve identification titles. There are 3 distinct anomalies: (1) the 298 K data for the c_{33} mode and the Q.L. mode deviates from a linear pressure-frequency relation at higher pressures; (2) the c_{44} mode frequencies, measured either by wave propagations parallel or perpendicular to the "c" axis initially decreases very slightly with pressure at 298 K but there is no net change between zero applied pressure and 3.03 kbar; (3) at 273 K the frequency for the c_{44} mode increases with initial pressure but no significant change occurs above 1 kbar.

The changes in wave velocity with pressure reflect the reductions in thickness of the crystals with increasing pressure as well as the basic frequency data given in Fig. 3. For both shear modes, c_{44} and c_{66} , the wave velocities have negative pressure coefficients at 298 K as well as 273 K. Since the density changes are inversely related to approximately the 3rd power of the change in thickness, all of the stiffness moduli have positive pressure coefficients. The effect of ferromagnetic ordering, as reflected in the differences between the 298 K and 273 K data, is to decrease the pressure coefficients of c_{11} , c_{33} , c_{13} and c_{66} whereas the pressure

coefficient of c_{44} is increased. The slopes of the linear parts of the pressure-modulus curves are given in Table II.

TABLE II
Pressure derivatives of adiabatic and isothermal c_{ij}

	$\frac{dc_{11}}{dp}$	$\frac{dc_{12}}{dp}$	$\frac{dc_{13}}{dp}$	$\frac{dc_{33}}{dp}$	$\frac{dc_{44}}{dp}$	$\frac{dc_{66}}{dp}$
Adiabatic 298 K	3.118	2.393	3.553	6.019	.07	.362
Isothermal 298 K	2.78	2.18	3.26	6.41		
Adiabatic 273 K	2.437	1.740	2.683	3.77	.29	.334
Isothermal 273 K	1.94	1.33	1.63	2.93		

The changes in adiabatic linear and volume compressibilities with pressure are given in Table III. The initial slope of the β_{11} vs pressure plot is about twice that for β_1 , at both 298 K and 273 K.

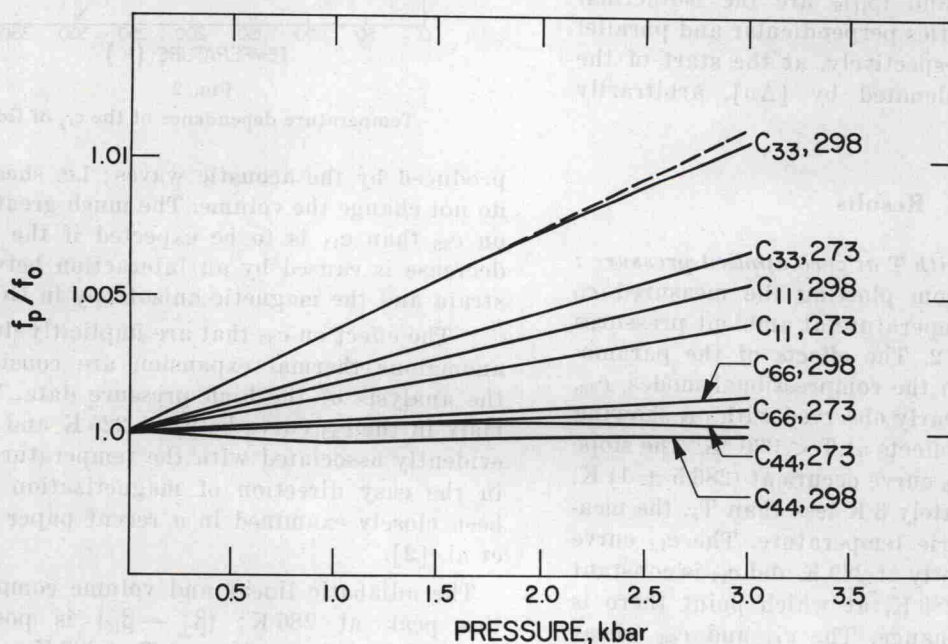


FIG. 3
Pressure dependence of the ratio of the pulse repetition rate frequency at pressure p , to that at one atmosphere for the propagation modes corresponding to the c_{ij} , at 298 K and 273 K.